

Nanoscale

Accepted Manuscript



This is an *Accepted Manuscript*, which has been through the Royal Society of Chemistry peer review process and has been accepted for publication.

Accepted Manuscripts are published online shortly after acceptance, before technical editing, formatting and proof reading. Using this free service, authors can make their results available to the community, in citable form, before we publish the edited article. We will replace this *Accepted Manuscript* with the edited and formatted *Advance Article* as soon as it is available.

You can find more information about *Accepted Manuscripts* in the [Information for Authors](#).

Please note that technical editing may introduce minor changes to the text and/or graphics, which may alter content. The journal's standard [Terms & Conditions](#) and the [Ethical guidelines](#) still apply. In no event shall the Royal Society of Chemistry be held responsible for any errors or omissions in this *Accepted Manuscript* or any consequences arising from the use of any information it contains.

ARTICLE

Intracellular delivery of peptide cargos using iron oxide based nanoparticles: studies on antitumor efficacy of BCL-2 converting peptide, NuBCP-9

Cite this: DOI:

10.1039/x0xx00000x

Manoj Kumar^a, Gurpal Singh^a, Sapna Sharma^a, Dikshi Gupta^a, Vivek Bansal^a, Vikas Arora^b, Madhusudan Bhat^c, Sandeep K. Srivastava^c, Sameer Sapra^b, Surender Kharbanda^d, Amit K. Dinda^c and Harpal Singh^{†a}

Received ooth XXXXXX

20XX,

Accepted ooth

XXXXXXXX20XX

DOI: 10.1039/x0xx00000x

www.rsc.org/

Abstract

Delivering peptides into cells targeting the undruggable oncoproteins, is an emerging area in cancer therapeutics. Here we report a novel nanoparticle-based delivery system that can transport therapeutic cargos to the intracellular sites without the need for a cell transduction or penetration domain (CPP). In the present study, we have used iron oxide nanoparticles to deliver an oncopeptide, NuBCP-9 targeting the BCL-2 BH3 domain. Citric acid/3bromomethylpropanoic acid (CA/BMPA)-capped SPIONs were used to immobilize and deliver NuBCP-9 peptide to the cancer cells without any noticeable off target effects. Our results have demonstrated that NuBCP-9-SPIONs are efficiently penetrate into cancer cells and binding to its intracellular target protein BCL-2. Moreover, significant inhibition of proliferation and substantial induction of cell death was observed when cancer cells were treated with NuBCP-9-SPIONs at different time intervals. Importantly, the IC₅₀ values for killing of breast cancer cells with NuBCP-9-SPIONs were much lower than compared to cells treated with NuBCP-9 peptide linked with a CPP (Arg-8; NuBCP-9-R8). Molecular and biochemical analysis further supported that NuBCP-9-SPIONs killed breast cancer cells by apoptosis-mediated mechanisms. Furthermore, our data demonstrated that administration of NuBCP-9-SPIONs to mice bearing ehrlich ascites tumors (EAT) was associated with loss of tumorigenicity and extensive apoptosis in tumor tissues. Taken together, these findings show that a non-CPP-tagged peptide can be successfully delivered to undruggable intracellular oncotargets using SPIONs.

Introduction

Members of the B-cell lymphoma-2 (BCL-2) protein family are critical regulators of apoptosis and include three subgroups of proteins which either promote cell survival (BCL-2, Bcl-xL, Mcl-1, Bcl-w), induce cell killing (Bim, Bid, PUMA) or activate the effector pathways of apoptosis (Bax, Bak). The discovery of BCL-2 established an important paradigm

in cancer biology that can also promote malignant transformation. The correct balance of activities, interaction and expression of these pro-survival or pro-apoptosis proteins are critical for cell survival and central to the initiation of apoptosis. Deregulated expression of BCL-2 or other members of this subgroup has been found to be a feature of many human cancers. There is a large body of evidence in the literature that indicate deregulated expression of BCL-2-like proteins

is a primary oncogenic event in tumor development and also causing therapeutic resistance¹⁻⁴. Thus targeting BCL-2 is an active area of research in cancer. To this context, a number of drugs targeting these oncoproteins are now undergoing clinical evaluations^{2, 4, 5}. One of the novel therapeutic approaches is the development of small molecule inhibitors that can directly target pro-survival BCL-2 family members. The most promising candidates are the small molecules ABT-737 and ABT-263 that are designed to target the hydrophobic pocket of BCL-2 or Bcl-xL⁶. Most of these drugs can freely pass through the plasma membranes and directly interact with mitochondrial-bound protein, BCL-2 [1].

Since small molecule inhibitors are often not specific for binding, recently several groups have focused on identifying peptide inhibitors that specifically bind to their targets. Therefore, development of anticancer peptides directed against intracellular onco-targets is currently a very promising area. However, delivery of anti-cancer peptides specifically into tumor cells is a major obstacle⁷. Several groups have used cell-penetrating peptides (CPP) or protein transduction domains (PTDs) to deliver specific peptides inside the tumor cells. CPPs are a class of short (8-40 amino acids) cationic peptides having universal capacity to breach biological membranes and enter cells, either alone or associated with cargo^{8, 9}. Recent studies have shown that a BCL-2-binding peptide (NuBCP-9; FSRSLHSLI) identified in Nur 77 protein, was able to bind to its target and efficiently kill tumor cells when delivered by using poly-Arg as PTD¹⁰.

Recent studies have described that NuBCP-9 act as molecular switch to induce a BCL-2 conformational change, converting it from a protector to a killer protein^{10, 11}. NuBCP-9 has a unique property that distinguishing it from other BCL-2 inhibitors under development. NuBCP-9 not only antagonizes the survival function of BCL-2 but also induces a BCL-2 conformation change that inhibits the survival function of its anti-apoptotic relatives, such as Bcl-X_L¹⁰. Moreover, NuBCP-9 peptide has anticancer activity without affecting the normal cells and thus has a strong potential to be used as a new generation anticancer agent for therapy. However, recently, Walkins et. al, have demonstrated that cooperative action of CPP with

NuBCP-9 cause cell membrane blebbing and necrosis. This cooperative action was found to be more pronounced in Dextro-NuBCP-9-r8 compared to its levo counterpart¹².

Over the past few years, nanotechnology has been shown the potential to dramatically impact the area of cancer drug delivery. In addition to liposomes, more recently, there has been interest in the development of therapeutic nanoparticles composed of either biodegradable polymers or iron oxide, which offer long circulation times. After administration, these therapeutic nanoparticles can selectively accumulate in tumor cells and thereby enhance the delivery of the drug payload to the site of disease. Nanoparticles accumulates into the tumor site by a mechanism known as enhanced permeability and retention (EPR) effect^{13, 14} thus enabling the site specific delivery¹⁵⁻¹⁷. The EPR effect occurs in tumors where the blood vessels are either disrupted or not fully formed and as a result are leakier than normal vessels. This phenomenon allows nanoparticles to pass readily from the blood vessels into the tumor and is differentially retained while the payload is released from the particles. Iron oxide NPs are widely studied for their potential applications in several fields¹⁸. Among all these applications, magnetic resonance imaging (MRI) and drug delivery are the major areas where these nanoparticles have been explored extensively¹⁹⁻²⁴. Site-specific delivery of chemotherapeutics, DNA, siRNA, proteins and peptide drugs is one of the promising applications of colloidal magnetic nanoparticles²⁵⁻²⁸.

Here we developed a multifunctional theranostic nanoparticles in which the L-amino acid NuBCP-9 (without poly-Arg tail; CPP/PTD; R denotes L-amino acid; r denotes D-amino) was conjugated with iron oxide nanoparticles involving bio-cleavable bond. These nanoparticles were used to overcome the problems related to the delivery of levo form of NuBCP-9 peptide to the interior of the tumor cells. The present results show that delivering the L-NuBCP-9 peptide by iron oxide nanoparticles blocks proliferation of the MCF-7 hormone-dependent breast carcinoma and HepG2 hepato carcinoma cells. The findings also show that intraperitoneal (IP) injection of iron oxide nanoparticles conjugated with NuBCP-9 peptide is

highly effective in the treatment of Ehrlich Ascites Tumor (EAT) model in mice.

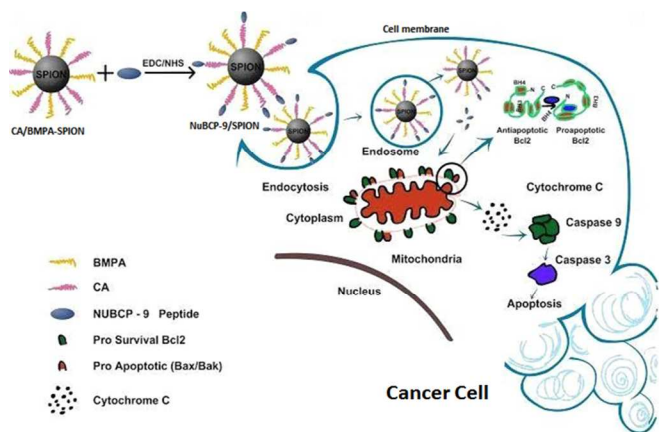


Figure 1. Schematic representation of bioconjugation and NuBCP-9 mediated killing of cancer cell overexpressing Bcl-2 by developed nanosystem (NuBCP-9-SPIONs).

Results and discussion

Nanosystem preparation

In the present study, we synthesized magnetic nanocrystals through the thermal decomposition method in organic solvent. Synthesized nanoparticles were characterized by different techniques (TEM, XRD, SQUID). The size of the nanoparticles ranges from 7-10nm and are superparamagnetic as confirmed from TEM and SQUID respectively (Electronic supplementary information; ESI-Figure S1). These nanoparticles are hydrophobic hence cannot be used in biological system therefore ligand exchange was performed using a combination of citric acid (CA)/2-Bromo2-methyl propionic acid (BMPA). CA/BMPA was able to replace the hydrophobic ligand completely from the surface of the nanoparticle without altering the properties of the nanoparticle. These nanoparticles are highly dispersible as shown in our previous studies²⁹. CA/BMPA capped SPIONs (CA/BMPA-SPIONs) were then used for conjugations with pro-apoptotic peptide, NuBCP-9 without CPP using EDC/NHS chemistry. Unconjugated NuBCP-9 was removed by ultrafiltration using 10KDa amikon filters (Millipore, USA). NuBCP-9-SPIONs were found to be monodispersed (7-10 nm), spherical and without any aggregation (Figure 2 inset

b). The zeta potential (ζ) measurement of nanoparticles was -33.0 and -40.6mV for SPIONs and NuBCP-9-SPIONs respectively. ATR-FTIR Spectra of NuBCP-9-SPIONs showed amide peak at 1642 cm^{-1} due to amide bond of NuBCP-9 confirming the conjugation of NuBCP-9 with SPIONs (Figure 1). The loading efficiency of the peptide was found to be $\sim 13.3 \pm 0.8\%$ wt % (NuBCP-9/Fe) using micro BCA assay.

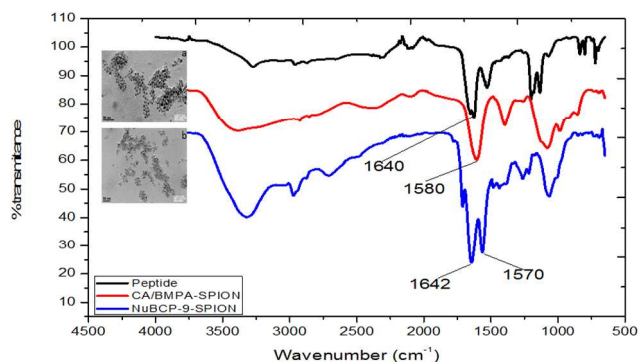


Figure 2 Comparative ATR-FTIR spectra of NuBCP-9, CA/BMPA-SPIONs and NuBCP-9-SPIONs (Inset, Transmission Electron Micrograph; a) CA/BMPA-SPIONs; b) NuBCP-9-SPIONs.

Cell Culture

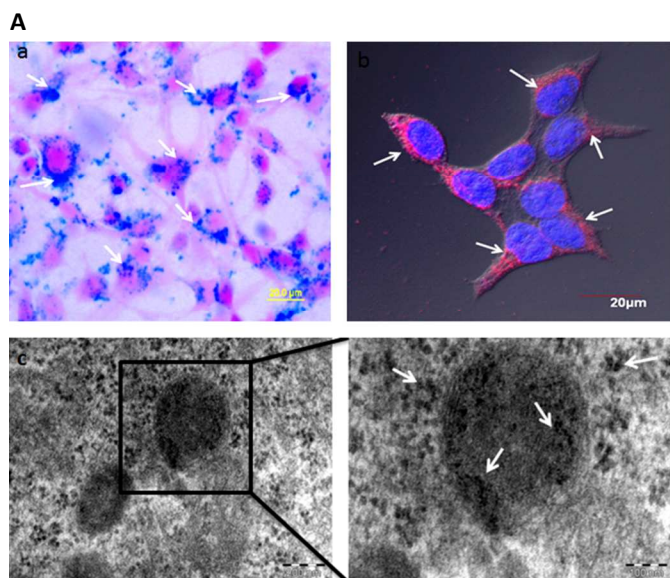
Cellular uptake studies

To demonstrate uptake of NuBCP-9-conjugated SPIONs by the tumor cells, multiple types of experiment were performed in hormone-dependent breast carcinoma cells, MCF-7. Firstly, the uptake of NuBCP-9-SPIONs was detected using Prussian blue staining which demonstrated that there was a substantial increase of intracellular iron, as visualized by blue granules in Prussian blue staining of MCF-7 cells (Figure 3A (a)). Furthermore, the uptake of RH-NuBCP-9-SPIONs (Rhodamine B tagged NuBCP-9-SPIONs) was demonstrated using CLSM showing intense red fluorescence of Rhodamine B while nuclei showed blue fluorescence due to DAPI staining (Figure 3A (b)). Additionally, TEM studies were performed in MCF-7 cells treated with NuBCP-9-SPIONs to evaluate ultra-structural characteristics. The results demonstrate localization of NuBCP-9-SPIONs inside the cells (Figure 3A (c)). Importantly, NuBCP-9-SPIONs were localized throughout the endosomes (Figure 3A (c) white arrows). We have observed numerous enlarged

endosomes in which NuBCP-9-SPIONs were accumulated. Further nanoparticles were also seen in the cytosol (Figure 3A (c) white arrows). Taken together, these findings indicated that NuBCP-9-SPIONs were effectively internalized by the tumor cells.

Co-localization of NuBCP-9-SPIONs with BCL-2

We evaluated the co-localizations of SPION-conjugated L-NuBCP-9 with BCL-2. These studies were performed by imaging the cells after treatment with RH-NuBCP-9-SPIONs followed by immunofluorescence staining of intracellular protein BCL-2. Figure 3B shows the fluorescence images of MCF-7 cells treated with RH-NuBCP-9-SPIONs. Merging the immunofluorescence images (orange/yellow) indicated a high level of co-localization between RH-NuBCP-9-SPIONs (Red) and BCL-2 (Green). These findings demonstrate significant binding between NuBCP-9 and BCL-2 (Figure 3B). Further, the intensity of binding of NuBCP-9-SPIONs with BCL-2 was calculated using image analysis software which shows Pearson's coefficient of 0.62%, indicating significant overlap between these two dyes. Importantly, our results also suggest that NuBCP-9 is binding with BCL-2 protein in the cytoplasm. Taken together, these observations imply that conjugating NuBCP-9 with SPIONs did not alter its binding ability with BCL-2 protein.



B

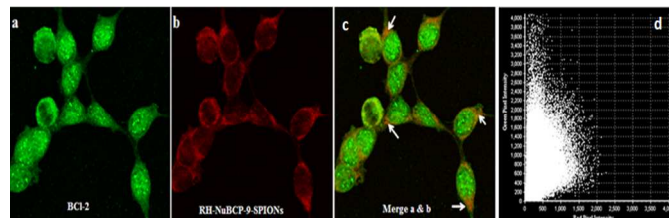


Figure 3. Cellular interaction studies A) cellular uptake studies of MCF-7 a) Prussian blue staining of MCF-7 cells treated with NuBCP-9-SPIONs; blue granules represent Fe while red stain represent nuclei of the cells b) Fluorescence staining of MCF-7 cell treated with Rhodamine B conjugated NuBCP-9-SPIONs; Red colour represent Rhodamine B conjugated NuBCP-9-SPIONs while blue colour represent nucleus stain with DAPI. (B) Colocalisation studies of NuBCP-9-SPIONs in MCF-7 cells a) Immunofluorescent staining of BCL-2 with antibodies (Green colour) b) cells were treated with rhodamine B conjugated NuBCP-9-SPIONs (Red colour) c) merge of image (a) and (b) d) Scatter plot of Pearson's correlation coefficient (r)

Effects of NuBCP-9-SPIONs on cancer cell growth and survival in vitro

To assess the biological activity, BCL-2-expressing MCF-7³⁰ or HepG2³¹ cells were treated with NuBCP-9-SPIONs and evaluated for proliferation. For comparison, primary HUVEC cells were also treated with NuBCP-9-SPIONs and the extent of proliferation was determined. As controls, MCF-7 and HepG2 cells were also separately treated with NuBCP-9 with and without the CPP domain. In contrast to L-NuBCP-9 without the poly-Arg, treating cells with 15 μ M NuBCP-9-R8 was associated with significant inhibition in proliferation (Fig 4). These findings confirmed the requirement of a CPP domain such as R8 for cell penetration. Importantly, treatment of cells with NuBCP-9 conjugated to SPIONs was associated with substantial inhibition of growth and thereby indicated that SPION conjugation effectively delivered the NuBCP-9 peptide into the cells. (Figure 4A and B). Moreover, SPIONs alone (not conjugated with NuBCP-9 peptide) had little if any effect on growth (Figure 4A and B). Interestingly, lack of growth inhibition by L-NuBCP-9-SPIONs in HUVEC cells indicated selective killing of BCL-2 overexpressing cancer cells (Figure 4E).

Additional studies were performed to assess the effects of NuBCP-9-SPIONs on cancer cell viability. As

expected, NuBCP-9-R8 induced death of MCF-7 and HepG2 cells in a dose-dependent manner (Figure 4C and D). Moreover, the NuBCP-9-SPIONs were also very effective in killing both the cell types (Figure 4C and D). Most importantly, L-NuBCP-9-SPIONs are much more potent than NuBCP-9-R8 as the IC_{50} values of NuBCP-9-SPIONs in MCF-7 and HepG2 was 1.32 and 2.31 μ M respectively while IC_{50} of NuBCP-9-r8 was 7.12 and 6.22 μ M. These results indicate that not only the NuBCP-9 peptide can be delivered intracellularly by SPIONs but also substantially reduce the IC_{50} for killing.

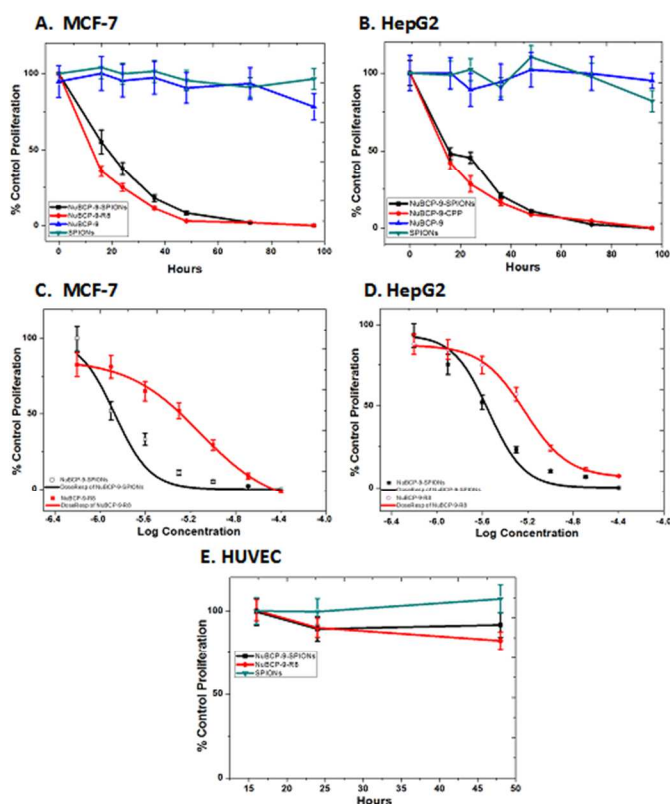


Figure 4. Effects of NuBCP-9 and NuBCP-9-SPIONs on cell proliferation. A. MCF-7 breast carcinoma cells were treated with SPIONs (cyan inverted triangles), 15 μ M NuBCP-9 (blue upward triangles), 15 μ M NuBCP-9-R8 (red circles), 15 μ M NuBCP-9-SPIONs (black squares) for the indicated times. B. HepG2 hepatocellular cancer cells were treated with SPIONs (cyan inverted triangles), 15 μ M NuBCP-9 (blue upward triangles), 15 μ M NuBCP-9-R8 (red circles), 15 μ M NuBCP-9-SPIONs (black squares) for the indicated times. C. MCF-7 cells were treated with different concentrations of NuBCP-9-R8 (red circles), NuBCP-9-

(black squares) for 72 h. D. HepG2 cells were treated with different concentrations of NuBCP-9-R8 (red circles), NuBCP-9-SPIONs (black squares) for 72 h. E. HUVEC cells were treated with 15 μ M NuBCP-9-R8 (cyan leftward triangles), 15 μ M NuBCP-9-SPIONs (black squares) for the indicated times. Cell proliferation was assessed by XTT assays. Results are expressed as mean \pm SE of three independent experiments.

NuBCP-9-SPIONs induce apoptosis of cancer cells

As reported, NuBCP-9-r8 is a selective inducer of cancer cell apoptosis by targeting BCL-2¹⁰. To assess the effects of NuBCP-9-SPIONs on the apoptotic response, MCF-7 cells were treated with NuBCP-9-SPIONs NPs and monitored for externalization of phosphatidylserine (PS) at the cell membrane. Confocal images of MCF-7 cells stained with Annexin V-Alexafluor 488/PI demonstrated that treatment with NuBCP-9-SPIONs was associated with the induction of an apoptotic response (Figure 5A). By contrast, treatment with plain SPIONs had no apparent effect (data not shown). Quantitation of annexin V and PI staining by Cellometer Vision confirmed that NuBCP-9-SPIONs are as effective as NuBCP-9-R8 in inducing apoptosis of MCF-7 cells at 48 h (Figure 5B). As additional control, NuBCP-9 devoid of r8 had little, if any, effect on MCF-7 cell apoptosis (Figure 5B). In concert with these results, treatment of MCF-7 and HepG2 cells with NuBCP-9-SPIONs was associated with activation of caspase-3 (Figure 5C). Collectively, these findings demonstrate that, conjugation of NuBCP-9 with SPIONs results in the induction of apoptosis of BCL-2-expressing carcinoma cells.

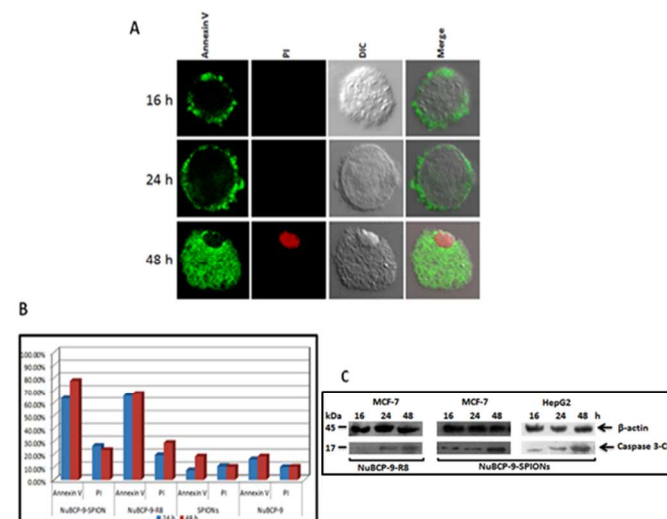


Figure 5. Measurement of apoptosis in Bcl-2 overexpressing cells **A)** Confocal laser scanning microscopic images of Annexin V and PI double staining of MCF-7 cells treated with (a) NuBCP-9-SPIONs for different times (a) 16 h (b) 24 h (c) 48 h. **B)** Quantification of Apoptosis/necrosis in MCF-7 cells by Annexin V/PI staining with treatment of NuBCP-9-SPIONs and NuBCP-9-R8 for 24 and 48 h using cellometer vision. Annexin V⁺/PI⁺ indicator of early apoptosis and AnnexinV⁺/PI⁺ late apoptotic/early necrotic. **C)** Expression of caspase 3 protein in the human Breast (MCF7), and hepato (HepG2) carcinoma cells by Western blot after treatment with 15 μ g/ml NuBCP-9 conjugated SPION's nanoparticles and NuBCP-9-R8 for 16,24,48 h.

Tumor inhibition studies

NuBCP-9-SPIONs are effective in inducing tumor regressions

To assess the anti-tumor effects of NuBCP-9-SPIONs in-vivo, we treated Balb/c mice bearing established (~400 mm³) subcutaneous Ehrlich syngeneic tumors overexpressing BCL-2³². Intraperitoneal (IP) injection of NuBCP-9 (devoid of R8) or empty SPIONs on a biweekly (1,3,7,10,14,18 and 21 d) schedule had no significant effect on tumor growth as compared to that obtained with the saline control (Figure 6). Significantly, IP treatment with L-NuBCP-9-SPIONs on the same schedule was associated with pronounced and significant tumor regressions (Figure 6). There was approximately 74% reduction in tumor volume in 21 days of injection in group treated with SPION formulation of NuBCP-9 (Figure 6).

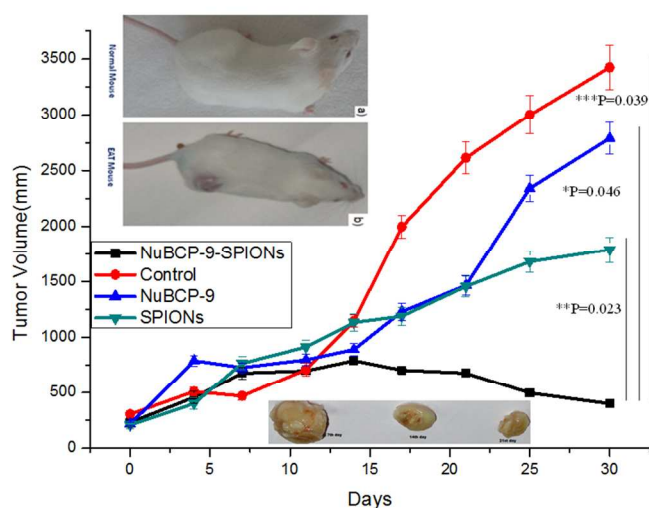


Figure 6. Anti-tumor activity of NuBCP-9/NPs. Therapeutic effects of NuBCP-9-SPIONs against EAT-

bearing mice and impact on tumor cell proliferation. Mice were treated bi-weekly for eight total doses with 20 mg/kg of NuBCP-9. Control mice received *NuBCP-9, **SPION and ***normal saline. A. Balb C mice orthotopically implanted in the left thigh with EAT cells were allowed to form tumors of approximately 200 mm³ in size and treated ~7th days after cells implantation. B, Regression of tumor growth in NuBCP-9-SPIONs treated mice along with different controls. Each point, mean \pm 95% CI of six replicates. C, Tumor mass removed from NuBCP-9-SPIONs on 7th, 14th and 21st days. $P < 0.05$ different from control EAT groups.

Importantly, following discontinuation of NuBCP-9-SPION at day 21, the tumors continue to regress and nearly complete tumor regressions were observed by 30 (Figure 6). Statistically analysis performed between different groups also demonstrated significant tumor regression in group treated with NuBCP-9-SPIONs compared to control groups ($p < 0.05$; * $p=0.046$; ** $p=0.023$; *** $p=0.039$). Importantly, there was no weight loss or other overt toxicities observed in L-NuBCP-9-SPIONs treated mice (data not shown). Other studies have also demonstrated regression in tumor in mice treated with chemotherapeutics conjugated with iron oxide nanoparticles.^{33, 34} Taken together, our studies have demonstrated that L-NuBCP-9 can be effectively delivered to tumor vasculature using SPIONs and importantly its conjugation with SPIONs caused regression of tumor without any toxicity. Studies are ongoing to evaluate the effects of L-NuBCP-9-SPIONs on BCL-2-expressing breast carcinoma xenografts in SCID-Nu/Nu mice.

Histopathology analysis

Tumors were harvested, formalin-fixed, paraffin-embedded, sectioned and subjected to histochemical examination. Tumors sections from L-NuBCP-9-SPION-treated mice were stained with H&E and Prussian blue. The results demonstrated different degree of necrosis and presence of blue patches representing Fe in tumor vasculature (Figure 7A). The histological examinations observed in the above biopsies clearly demonstrated that the inoculated tumor cells have varying degree of necrosis. Figure 7A showed the H&E staining of tumor tissues of mice treated with L-NuBCP-9-SPIONs and SPIONs after 7th, 14th and 21st days. H&E staining of the tumor tissue

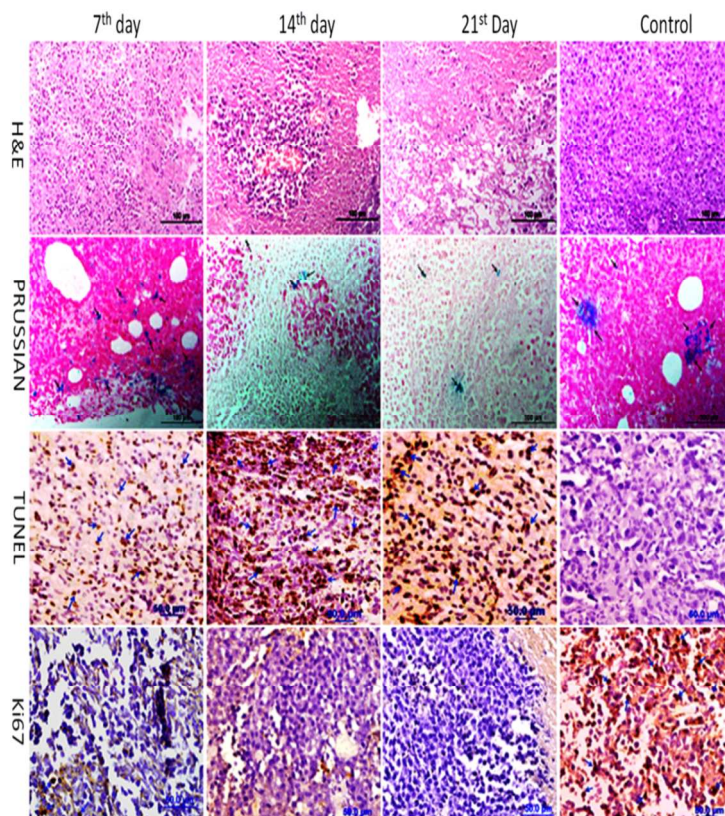
showed as variably sized regions containing necrotic tissue (cell fragments, nuclear debris and/or pyknotic cells) interspersed between regions of viable tumor cells. The severity of necrosis decreased radially from the center, with all tumors demonstrating necrosis deep in their centres. The host tissue adjacent to the growing edge of the tumor showed mild inflammatory cell infiltration. In the viable portion of the tumor at 7 and 14 days of tumor cells had large hypochromatic irregular shape of nuclei and adequate amount of cytoplasm. The mitotic figures were seen dispersed randomly throughout the growing edge of the tumor. Similarly at 21st day, the tumor nuclei appear more hypochromatic with lesser cytoplasmic content. It was also observed that the varying degree of necrosis was present in group treated with nanoformulation which increases with time from 7th to 21st days. Lowest necrotic proportions were observed in tumors of control samples as compared to NuBCP-9-SPIONs treated tumors.

The sections stained with Prussian blue staining showed (Figure 7A) presence of Fe within the tissue samples which varied with time, it was more in tumor with 7th day and lesser in 21 days. This study revealed that SPIONs with peptide had interspersed in the tumor tissue through blood, endocytosed by tumor cells and the conjugated peptide leads to apoptosis/necrosis in the target tissue. The NuBCP-9-SPIONs did not have the targeting moiety but they achieved the passive targeting due to fenestrated tumor vasculature. The lesser blue granules, which were observed in tumor tissue after 21 days of injection can be explained by the fact that iron oxide nanoparticles degrade in biological environment³⁵.

We also evaluated the effect of NuBCP-9-SPIONs on cell proliferation and apoptosis by Ki-67 and TUNEL (terminal deoxynucleotidyl transferase-mediated dUTP nick-end labeling) staining for proliferation and apoptosis, respectively. Tumors were harvested, formalin-fixed, paraffin-embedded, sectioned and subjected to immunohistochemistry. NuBCP-9-SPIONs-treated EAT bearing mice showed decreased expression of Ki-67. The decrease in expression of Ki-67 was observed from 7th day till 21 days in animals treated with NuBCP-9-SPIONs compared to group treated with plain SPIONs. The proliferative indices of

the different groups showing Ki-67 expression are given in Figure 7A. Control tumors contain hypercellular areas with a high expression of Ki-67. The level of apoptosis in tumors is confirmed by TUNEL assays.

A. Histology and Immunostaining



B. Apoptotic and Proliferative Index

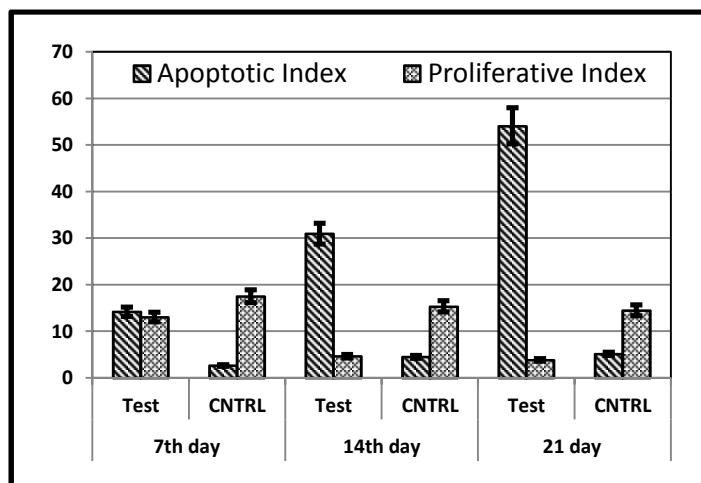


Figure 6 Histology and immunohistochemical staining of

tumor tissue. High power photomicrograph of H & E, Prussian blue, TUNEL staining and Ki67 staining of tumor tissue of NuBCP-9-SPION treated after different intervals of time (i) 7th day (ii) 14th day (iii) 21st day along with control.

A progressive increase in apoptotic cells (TUNEL +ve tumor cells) were detected in the NuBCP-9-SPIONs treated group to that compared with control. This can be attributed to effect of NuBCP-9-SPIONs on inhibition of tumor cell proliferation with concomitant induction of tumor cell apoptosis. Furthermore, we have also calculated the apoptotic index by counting the TUNEL positive nuclei which suggest that there is increase in apoptotic cells from 7th to 21st day in treated group compare to that with control group. We have also calculated ratio of proliferative/ apoptotic index of the EAT tumor tissues of NuBCP-9-SPIONs treated groups which also indicated the progressive tumor cell death in the nanoformulation treated group. All these results indicate that NuBCP-9-SPIONs based nanoformulation can promote apoptosis in tumor cells of EAT bearing mice and leads to reduce the tumor burden in treated animals. Based on TUNEL and Ki-67 staining apoptotic and proliferative indices in the tumor tissue was also calculated (Figure 6B). The apoptotic index in tumor tissue of control animals remains around between 3.17 ± 0.76 to 4.02 ± 1.89 while the proliferative index of these animals ranges between 10.18 ± 1.17 to 14.77 ± 2.48 . In contrast, NuBCP-9-SPIONs treated animals tumor shows higher apoptotic index which increased from $14.19\% \pm 1.99\%$ to $54.64\% \pm 4.66\%$ while proliferative index decreased from $9.88\% \pm 2.01\%$ to $3.83\% \pm 0.46\%$ from 7th - 21st day. Additionally, the ratio of proliferative and apoptotic index suggest that there is a decrease in proliferation and increase in apoptosis (~16 fold). Taken together, these results suggest that treatment of EAT bearing mice with NuBCP-9-SPIONs was associated with substantial regression of tumors to that compared with plain SPIONs and the killing of tumors cells was in part mediated by apoptosis.

Target specificity of peptide drugs in comparison to small molecules, have significant potential for targeting the undruggable intracellular onco-targets³⁶. To this context, several studies have shown in the recent past that peptide-based

drugs are under different stages of development. Few examples are: i) survivin³⁷; ii) HDM2³⁸ iii) NOTCH³⁹; iv) MUC1⁴⁰; v) β -catenin⁴¹, among others. B-cell lymphoma-2 (BCL-2) protein has been shown as a promising target for oncology. BCL-2 protein has also been shown to be substantially upregulated in cancers especially in relapsed and refractory conditions. Therefore, BCL-2 protein has also been the focus of peptide inhibitor development. To this context, many strategies are ongoing for targeting BCL-2 protein such as: using stabilized alpha-helices of BCL-2 domains (SAHBs)⁴². Earlier studies have shown that BCL-2 protein can be converted from an anti-apoptotic protein to an inducer of cell death by the Nur77-derived NuBCP-9 peptide^{10,43}. Although peptide-based therapeutics is selective and target-specific as compared with small molecule inhibitors, however the intracellular delivery of peptide drugs is a major challenge. Delivery of peptides required the inclusion of a cell or protein transduction domain (CTD/PTD) for intracellular delivery⁴⁴. To this context, NuBCP-9 was linked to the CPP D-Arg octamer (r8)¹⁰. The results in that study clearly demonstrate that treatment of tumor cells in vitro with NuBCP-9-r8 effectively kills¹⁰. Additionally, intra-tumoral injections of NuBCP-9-r8 to tumor-bearing mice is also effective in inducing apoptosis in vivo¹⁰. Intra-tumoral injection is not a feasible route of administration for humans and hence a challenge for the development of many peptide drugs, like NuBCP-9, is the issue of systemic delivery. Additionally, injecting peptide drugs intravenously can be limited by pharmacologic parameters, such as short circulating half-lives and hence necessitated frequent daily dosing for effective anti-tumor activity in xenograft tumor models⁴⁰. In the present study using BCL-2-interacting NuBCP-9 peptide as a model, we have generated supramagenetic iron oxide nanoparticles (SPIONs) and characterized the delivery and assessed the efficacy in vitro and in vivo. Encapsulation or immobilization of drugs in nanoparticles are being widely used for the effective delivery of small molecules.^{45, 46} Recently, we have effectively delivered L- amino acid of NuBCP-9 (without PTD/ CPP) to the intracellular oncotargets BCL-2 in-vitro and in-vivo using polymeric nanocarriers⁴⁷. Among different nanoparticles, magnetic nanoparticles possess unique

magnetic properties and can serve both as contrast enhancement agent in MRI and as a drug carrier in controlled drug delivery, targeted at cancer diagnosis and therapy^{48, 49}. An effective method of diagnosis and therapeutic application is to conjugate SPIONs with therapeutic drugs. Number of chemotherapeutic drugs has been delivered using SPIONs⁴⁹⁻⁵¹. However, the collective experience to deliver peptides through SPIONs is very much limited. In addition, a highly toxic mitochondria-targeted D[KLAKLAK]2 peptide as the drug to target glioblastoma have been delivered using SPIONs wherein iron oxide also served as diagnostic component for MRI⁵². To our knowledge, none of these peptide nanoformulations have been further developed for clinical evaluation.

In the present study, the SPIONs were generated using a thermal decomposition method followed by its ligand exchange using a combination of CA/BMPA²⁹. The advantage of using these small ligands did not increase the particle size significantly. Our previous studies reported that these nanocrystals have very good MRI contrast properties and can be used for diagnosis of cancers. In this regard, conjugating peptide drug on these nanoparticles make them as potential candidate for diagnosis and therapeutics of cancer. These findings are therefore of potential significance for the development of these NPs as theranostics agents for clinical applications. Cellular studies have shown the effective uptake of NuBCP-9-SPIONs and conjugating NuBCP-9 on to SPIONs surface did not alter its binding ability to BCL-2 protein in the cytosol of the cell overexpressing BCL-2. Our studies indicated that SPIONs can deliver NuBCP-9 effectively into cytosol probably due to endocytosis without affecting the biological activity of the peptide. These findings collectively indicate that NuBCP-9-SPIONs can deliver the active form of peptide into the cell without the requirement of a cell transduction domain.

NuBCP-9 is a highly promising anti-cancer peptide that selectively induces apoptosis of cancer cells by exposing the BCL-2 BH3 domain and blocking the Bcl-xL survival function.¹⁰ NuBCP-9 was linked to the D-Arg octamer r8 for intracellular delivery, a modification that has been reported to decrease selectivity by inducing BCL-2-independent cell killing involving membrane disruption¹². In the present work,

delivery of L-NuBCP-9 into cancer cells by SPIONs was achieved without the need for the r8 cell transduction domain. In addition, NuBCP-9-SPIONs were by comparison more potent in inducing apoptosis than NuBCP-9-R8. NuBCP-9-SPIONs also maintained the reported selectivity of NuBCP-9 for cancer cells as evidenced by their absence of HUVEC killing. Previous studies of the anti-tumor effects of NuBCP-9-r8 in vivo were performed by direct injection of NuBCP-9-r8 into MDA-MB-435 breast cancer xenografts in SCID mice¹⁰. Under these experimental conditions, NuBCP-9-r8 treatment was associated with partial MDA-MB-435 tumor regressions¹⁰. Importantly, in the present studies using the subcutaneous Ehrlich tumor model in syngeneic mice, we studied the effectiveness of NuBCP-9-SPIONs administered intraperitoneally (IP). Significantly, NuBCP-9-SPIONs administrations were effective in inducing pronounced regressions of the Ehrlich tumors. Significant number of apoptotic bodies were observed in the tumor tissue that increases with time in groups treated with NuBCP-9-SPIONs while proliferative markers reduces with time, indicating the specificity and efficacy of the nanoformulation. Of further importance, administration of the NuBCP-9-SPIONs was well tolerated with no evidence of weight loss or overt toxicities. These results thus provide support for the effective delivery of L-amino acid NuBCP-9 by SPIONs and may be applicable to other anti-cancer peptides and these nanoformulations can be developed for theranostics applications. Furthermore, it was also established from these studies that major limitations for systemic delivery of the therapeutic peptide particularly in cancer therapy was addressed, also the therapeutic potential of the peptide was maintained at the tumor site and better tumor penetration was achieved by use of tailored nanoformulation.

Experimental

Materials and methods

NuBCP-9 was custom synthesized from Bioconcept Pvt. Ltd, Maneser, Haryana. 1-Ethyl-3-(3-Diethyl aminopropyl)-Carbodimide (EDC) and N-hydroxysuccinamide (NHS), propidium iodide and Tris-HCl were purchased from Sigma Aldrich (USA). EAT cells were obtained from Institute of Nuclear Medicine

and Allied Sciences (INMAS), New Delhi. XTT cell proliferation kit was purchased from Cayman, USA. Tween 20 was purchased from Merck India. Hematoxylin and Eosin were purchased from Bio Lab Diagnostics India Private Limited.

Synthesis and hydrophilization of SPIONs

Synthesis and ligand exchange (CA/BMPA) of superparamagnetic iron oxide nanoparticles (SPIONs) was done as reported previously²⁹. Synthesized nanoparticles were characterized using TEM (Philips, Model CM12), XRD (Philips 1820 X-ray diffractometer using Cu K α radiation), SQUID (Quantum Design Ever Cool MPMS XL-7), Nanoparticles tracking analysis (NS500, Nano sight, UK) and ATR-FTIR (Spectrum one, Perkin Elmer, UK).

Bioconjugation and immobilization efficiency of SPIONs

NuBCP-9 was conjugated to CA/BMPA-SPIONs as reported previously^{29, 53, 54}. For conjugation, 10 mg of dried CA/BMPA coated SPIONs were dispersed in PBS buffer pH 7.4 and then treated with EDC (340 μ l, 400mM) and NHS (340 μ l, 100mM) and the mixture was gently shaken for 20 min. After this, 2mg of NuBCP-9 in PBS (pH-7.4) was added and the solution was gently shaken for another 1 h followed by ultrafiltration using 10 KDa (Amicon filters, Millipore, USA) filters to remove unreacted NuBCP-9 which comes in the filtrate. This step was repeated for 2-3 times for complete removal of unreacted NuBCP-9 and other impurities. The morphology and confirmation of conjugation of NuBCP-9 with SPIONs was done with TEM and ATR-FTIR.

Immobilization efficiency of NuBCP-9 in SPIONs was measured by Bicinchonic Assay (BCA) kit (Pierce, USA). Filtrate and peptide stock used for conjugation was analyzed for protein content using micro BCA kit as per manufacturer instructions. The encapsulation efficiency was calculated by the following equation⁵⁵.

$$\text{Immobilization efficiency (\%)} = ([\text{Peptide}]_{\text{tot}} - [\text{Peptide}]_{\text{filtrate}}) / [\text{Peptide}]_{\text{tot}} \times 100$$

Cell culture

MCF-7 (hormone-dependent breast carcinoma) and HepG2 (hepto-carcinoma) cells were obtained from NCCS, Pune, India. The cells were maintained in

DMEM medium supplemented with 10% fetal bovine serum and 100 mg/mL penicillin G and 100 mg/ml streptomycin (Gibco BRL, Grand Island, NY) in an incubator (Thermo fisher scientific MA, USA) at 37^oC in a humidified and 5% CO₂ atmosphere.

Cellular uptake study

Intracellular uptake of NuBCP-9-SPIONs was done with three methods, a) Prussian blue staining b) Florescence and c) TEM study. Prussian blue and florescence staining, 5 \times 10⁴ cells were seeded on coverslips in twelve well culture plates and grown for 24 hours. Cells were treated with NuBCP-9-SPIONs and RH-NuBCP-9-SPIONs separately with peptide concentrations (NuBCP-9) of 15 μ M for Prussian blue and florescence staining respectively. After incubation for 8 hours, the coverslips were removed followed by washing with phosphate buffer saline (PBS) solution and finally fixed with 4% paraformaldehyde for 20 minutes at room temperature. Prussian blue staining was done as reported previously²⁹ and florescence stained samples were treated with DAPI. Finally all slides were observed under microscope (Olympus, Fluoview FV1000 Microscope, Japan).

c) Transmission electron microscopy (TEM) study. MCF-7 cells were grown in twelve well cell culture plates. After 24 hours, NuBCP-9-SPIONs (15 μ M peptide concentration) were added and incubated for 8 hours and the rest of the procedure was performed according to Zhou et al.⁵⁶ Finally, samples were viewed under an electron microscope (Morgagni 268; Philips, Amsterdam, Netherlands).

Colocalization experiment and confocal microscopy

These experiments were performed on human breast cancer (MCF-7) cells. Cells grown on glass cover slips to 50–60% cell density and then treated with RH-NuBCP-9-SPIONs (red colour) for 8 hours at 37 $^{\circ}$ C in a humidified 5% CO₂-95% air incubator chamber and were then washed and fixed in 4% paraformaldehyde in PBS (pH 7.2) supplemented with 0.01% glutaraldehyde for 1.5 h followed by extensive washing with 1XPBS.

PBS was aspirated and coverslips were covered with methanol. Cells were allowed to fix for 15 minutes at room temperature. Methanol was aspirated and rinsing was done with PBS. Coverslips were blocked with

blocking buffer for 60 minutes. Cells were then incubated at overnight, 4 °C, with anti-BCL-2 antibodies (Santa Cruz Biotechnology, Inc, USA) in 1% FBS-PBS. After incubation samples were washed three times in PBS for 5 minutes each and then incubated with FITC-conjugated secondary antibody (Vector laboratories, USA) for 30 minutes at room temperature in dark. After removal of nonreactive Antibody and extensive washing, the cover slips were mounted on glass slides over Prolong Gold Antifade 1922 (Life technologies, USA) and examined under Confocal Laser Scanning Microscope (Olympus, Fluoview FV1000 Microscope, Japan). The colocalization of the peptide and BCL-2 was confirmed by overlapping green (anti-BCL-2) and red (RH-NuBCP-9-SPIONs) fluorescent labels that produced yellow fluorescence (combined green and red fluorescence).

Proliferation inhibition studies of NuBCP-9 in different cell lines

To determine the effect of encapsulated NuBCP-9 on cell proliferation, cancer cell lines (MCF-7 and HepG2) were treated with NuBCP-9, NuBCP-9-R8, SPIONs and NuBCP-9-SPIONs for different time intervals (16 -96 h) using the XTT based in-vitro toxicology assay kit (Cayman, USA). Similar experiments were also performed using multiple concentrations of these test articles (0.625-40 µM). Cells (2.5×10^3) were seeded in 96 well culture plates and incubated for 24 h followed by treatment with different NuBCP-9 formulations. After incubation, medium was aspirated from the culture wells and 100 µl of fresh media was added followed by addition of 10 µl of XTT reagent. Plates were incubated at 37°C for 4 h as per manufacturer's instructions. Following 4 h of incubation, absorbance was measured at 450 nm with reference wavelength of 630 nm using ELISA plate reader. Cell proliferation activity was determined by comparing the control samples with the treated samples. Half maximal inhibitory concentration (IC_{50}) values were calculated using Origin 8.0 (Origin Lab Corporation, Northampton, MA, USA).

Assessment of apoptosis

Cells were stained using the Annexin V-Alexa Fluor 488/PI Apoptosis Assay Kit (Invitrogen). Quantification

of apoptosis/necrosis was performed using Cellometer Vision (Nexcelom Bioscience LLC). Cells were also imaged using the CLSM microscope.

Immunoblot analysis

Cell lysates were prepared with M-PER reagent (Pierce Chemicals) and analyzed by immunoblotting with anti-BCL-2, anti-caspase-3 (Santa Cruz Biotechnology) and anti-β-actin (Sigma).

Animal studies

Balb c mice (17-22 g, AIIMS, Delhi) were used for in-vivo experiment and ethical clearance was obtained from CPCSCA committee (IAEC/611/2011). All of the procedures complied with the standards for humane care and use of animal subjects as stated in, The Guide for the Care and Use of Laboratory Animals.

Ehrlich solid tumor regression studies

Erlich Ascitic Tumor (EAT) cells (5×10^6 cells/mice) were injected into the right hind limb (thigh) of all the animals (Balb C mice) subcutaneously to generate solid tumor and were divided into four different groups (n=6). Three groups received treatment of NuBCP-9-SPIONs, *NuBCP-9 and **SPIONs by intraperitoneal route with biweekly injections of peptide concentration of 20 mg/kg/mice and fourth group of mice were injected with ***normal saline (NS) only. The treatments were started from day 7th of tumor implantation and continued upto 21st day. From each group, 3 animals were sacrificed at day 7th, 14th and 21st and tumor tissue was removed, weighed, tabulated and preserved in buffered formalin and processed for histopathological investigations. Tumor volume was determined using external caliper, the greatest longitudinal diameter (length) and the greatest transverse diameter (breadth) was also determined. Tumor volume based on caliper measurements were calculated by the modified ellipsoidal formula^{57, 58}

$$Tumor\ volume = 1/2 \cdot length \times breadth^2$$

The tumor growth inhibition (TGI)⁵⁹ was also calculated by the following equation:

$$TGI = \frac{V\ of\ SPIONs\ control\ group - V\ of\ tested\ group}{V\ of\ SPIONs\ control\ group} \times 100$$

Where V is means the average of tumor volume.

Histology and Immunohistology

Portions of tumor tissue was fixed in 10% buffered formalin-saline at 4°C overnight and then embedded in paraffin blocks. Tissue sections of 5 µm thickness were stained with Hematoxylin and Eosin (H&E) and Prussian blue staining.

Analysis of NuBCP-9-SPIONs on proliferation of EAT mice tumors was performed using Ki-67 antibody. Tissue specimens were processed for immunohistochemical analyses as described previously⁶⁰. The tumor sections were deparaffinized and immersed in 10 mM citrate buffer. Heat-induced antigen retrieval was accomplished in a pressure cooker. Endogenous peroxidase activity was quenched with 3% hydrogen peroxide. To reduce non-specific staining, the sections were incubated with 10% normal goat or rabbit serum. After overnight treatment with anti-mouse monoclonal Ki-67 antibody (Abcam, MA, USA), sections were incubated with biotinylated secondary antibody and streptavidin-biotin-peroxidase complex (SABC), sequentially. The immunoreaction was visualized using the diaminobenzidine (DAB) solution as the chromogen, and followed by counterstaining with Mayer's hematoxylin.

Evaluation of Cell Apoptosis in Tumor Tissues

Tumor tissues were stained with tunnel staining kit as per manufacturer protocol (In situ death detection kit, POD, Roche, Germany). Finally stained sections were observed by microscope (Olympus, Fluoview FV1000 Microscope, Japan). To determine the apoptotic and proliferative indices, six fields were chosen randomly and analyzed to calculate the proliferative or apoptotic index as follows:

$$\text{Proliferative index/apoptotic index (\%)} = 100 \times \frac{\text{proliferative/apoptotic cells}}{\text{total tumor cells}}$$

Statistical Analysis

Data were analyzed by two-tailed Student's unpaired t test. P values of <0.05 were considered statistically significant.

Conclusions

In summary, our findings describe a novel iron oxide nanoparticle-based approach for delivery of L-amino acid peptides without a cell-penetrating domain that (i) can be delivered through nanocrystals, (ii) can be used for diagnosis and treatment (theranostics), (iii) induces effective anti-cancer activity in vitro and in vivo and (iv) requires less frequent dosing (twice/week) compared to the daily injections that were necessary for anti-tumor activity of the D-amino acid NuBCP-9-r8 peptide in vivo¹⁰.

Acknowledgements

The authors gratefully acknowledge Department of Science and Technology, Govt. of India for financial supported.

Notes and references

^aCenter for Biomedical Engineering, Indian Institute of Technology, Delhi, Hauz Khas, New Delhi- 110016, India

Tel: +91-26591149; Email: harpal2000@yahoo.com

^bDepartment of Chemistry, Indian Institute of Technology, Delhi, Hauz Khas, New Delhi-110016, India

^cDepartment of Pathology, All India Institute of Medical Sciences Ansari Nagar, New Delhi- 110023, India.

^dDepartment of Medical Oncology, Dana-Farber Cancer Institute, Harvard Medical School, Boston, MA 02115, USA

† Footnotes should appear here. These might include comments relevant to but not central to the matter under discussion, limited experimental and spectral data, and crystallographic data.

Electronic Supplementary Information (ESI) available: [details of any supplementary information available should be included here]. See DOI: 10.1039/b000000x/

1. A. Ashkenazi, *Nature Reviews Drug Discovery*, 2008, **7**, 1001-1012.
2. E. C. Borden, H. Kluger and J. Crowley, *Nature Reviews Drug Discovery*, 2008, **7**, 959-959.
3. T. G. Cotter, *Nature Reviews Cancer*, 2009, **9**, 501-507.

4. K. W. Yip and J. C. Reed, *Oncogene*, 2008, **27**, 6398-6406.
5. G. Szakacs, J. K. Paterson, J. A. Ludwig, C. Booth-Genthe and M. M. Gottesman, *Nature Reviews Drug Discovery*, 2006, **5**, 219-234.
6. T. Oltersdorf, S. W. Elmore, A. R. Shoemaker, R. C. Armstrong, D. J. Augeri, B. A. Belli, M. Bruncko, T. L. Deckwerth, J. Dinges, P. J. Hajduk, M. K. Joseph, S. Kitada, S. J. Korsmeyer, A. R. Kunzer, A. Letai, C. Li, M. J. Mitten, D. G. Nettesheim, S. Ng, P. M. Nimmer, J. M. O'Connor, A. Oleksijew, A. M. Petros, J. C. Reed, W. Shen, S. K. Tahir, C. B. Thompson, K. J. Tomaselli, B. Wang, M. D. Wendt, H. Zhang, S. W. Fesik and S. H. Rosenberg, *Nature*, 2005, **435**, 677-681.
7. A. T. Jones, *International Journal of Pharmaceutics*, 2008, **354**, 34-38.
8. M. Grdisa, *Current Medicinal Chemistry*, 2011, **18**, 1373-1379.
9. C. Foged and H. M. Nielsen, *Expert Opinion on Drug Delivery*, 2008, **5**, 105-117.
10. S. K. Kolluri, X. W. Zhu, X. Zhou, B. Z. Lin, Y. Chen, K. Sun, X. F. Tian, J. Town, X. H. Cao, F. Lin, D. Y. Zhai, S. Kitada, F. Luciano, E. O'Donnell, Y. Cao, F. He, J. L. Lin, J. C. Reed, A. C. Satterthwait and X. K. Zhang, *Cancer Cell*, 2008, **14**, 285-298.
11. F. Luciano, M. Krajewska, P. Ortiz-Rubio, S. Krajewski, D. Y. Zhai, B. Faustin, J. M. Bruey, B. Bailly-Maitre, A. Lichtenstein, S. K. Kolluri, A. C. Satterthwait, X. K. Zhang and J. C. Reed, *Blood*, 2007, **109**, 3849-3855.
12. C. L. Watkins, E. J. Sayers, C. Allender, D. Barrow, C. Fegan, P. Brennan and A. T. Jones, *Molecular Therapy*, 2011, **19**, 2124-2132.
13. A. A. Manzoor, L. H. Lindner, C. D. Landon, J. Y. Park, A. J. Simnick, M. R. Dreher, S. Das, G. Hanna, W. Park, A. Chilkoti, G. A. Koning, T. L. M. ten Hagen, D. Needham and M. W. Dewhirst, *Cancer Research*, 2012, **72**, 5566-5575.
14. Y. Matsumura and H. Maeda, *Cancer Research*, 1986, **46**, 6387-6392.
15. R. Gref, Y. Minamitake, M. T. Peracchia, V. Trubetskoy, V. Torchilin and R. Langer, *Science*, 1994, **263**, 1600-1603.
16. X. Y. Zhang, J. Chen, Y. F. Zheng, X. L. Gao, Y. Kang, J. C. Liu, M. J. Cheng, H. Sun and C. J. Xu, *Cancer Research*, 2009, **69**, 6506-6514.
17. A. Vila, A. Sanchez, M. Tobio, P. Calvo and M. J. Alonso, *Journal of Controlled Release*, 2002, **78**, 15-24.
18. D. E. Lee, H. Koo, I. C. Sun, J. H. Ryu, K. Kim and I. C. Kwon, *Chemical Society Reviews*, 2012, **41**, 2656-2672.
19. J. W. M. Bulte and D. L. Kraitchman, *Nmr in Biomedicine*, 2004, **17**, 484-499.
20. A. Jedlovszky-Hajdu, E. Tombacz, I. Banyai, M. Babos and A. Palko, *Journal of Magnetism and Magnetic Materials*, 2012, **324**, 3173-3180.
21. F. Sonvico, S. Mornet, S. Vasseur, C. Dubernet, D. Jaillard, J. Degrouard, J. Hoebeke, E. Duguet, P. Colombo and P. Couvreur, *Bioconjugate Chemistry*, 2005, **16**, 1181-1188.
22. J. Zhang, S. Rana, R. S. Srivastava and R. D. K. Misra, *Acta Biomaterialia*, 2008, **4**, 40-48.
23. J. R. Hwu, Y. S. Lin, T. Josephrajan, M. H. Hsu, F. Y. Cheng, C. S. Yeh, W. C. Su and D. B. Shieh, *Journal of the American Chemical Society*, 2009, **131**, 66-+.
24. P. C. Wu, W. S. Wang, Y. T. Huang, H. S. Sheu, Y. W. Lo, T. L. Tsai, D. B. Shieh and C. S. Yeh, *Chemistry-a European Journal*, 2007, **13**, 3878-3885.
25. J. Chomoucka, J. Drbohlavova, D. Huska, V. Adam, R. Kizek and J. Hubalek, *Pharmacological Research*, 2010, **62**, 144-149.
26. M. Mahmoudi, S. Sant, B. Wang, S. Laurent and T. Sen, *Advanced Drug Delivery Reviews*, 2011, **63**, 24-46.
27. C. Sun, J. S. H. Lee and M. Q. Zhang, *Advanced Drug Delivery Reviews*, 2008, **60**, 1252-1265.
28. N. Tran and T. J. Webster, *Journal of Materials Chemistry*, 2010, **20**, 8760-8767.

29. M. Kumar, G. Singh, V. Arora, S. Mewar, U. Sharma, N. Jagannathan, S. Sapra, A. K. Dinda, S. Kharbanda and H. Singh, *Int J Nanomedicine*, 2012, **7**, 3503-3516.
30. B. Nathan, B. Gusterson, D. Jadayel, M. O'Hare, R. Anbazhagan, H. Jayatilake, S. Ebbs, K. Micklem, K. Price, R. Gelber and et al., *Ann Oncol*, 1994, **5**, 409-414.
31. J. Tan, B. Wang and L. Zhu, *Chem Biodivers*, 2009, **6**, 1101-1110.
32. A. Bhattacharyya, T. Choudhuri, S. Pal, S. Chattopadhyay, G. K. Datta, G. Sa and T. Das, *Carcinogenesis*, 2003, **24**, 75-80.
33. C. N. Zhang, W. Wang, T. Liu, Y. K. Wu, H. Guo, P. Wang, Q. Tian, Y. M. Wang and Z. Yuan, *Biomaterials*, 2012, **33**, 2187-2196.
34. M. K. Yu, Y. Y. Jeong, J. Park, S. Park, J. W. Kim, J. J. Min, K. Kim and S. Jon, *Angewandte Chemie-International Edition*, 2008, **47**, 5362-5365.
35. T. K. Jain, M. K. Reddy, M. A. Morales, D. L. Leslie-Pelecky and V. Labhasetwar, *Molecular Pharmaceutics*, 2008, **5**, 316-327.
36. G. L. Verdine and L. D. Walensky, *Clin Cancer Res*, 2007, **13**, 7264-7270.
37. J. Plescia, W. Salz, F. Xia, M. Pennati, N. Zaffaroni, M. G. Daidone, M. Meli, T. Dohi, P. Fortugno, Y. Nefedova, D. I. Gabrilovich, G. Colombo and D. C. Altieri, *Cancer Cell*, 2005, **7**, 457-468.
38. E. Sarafray-Yazdi, W. B. Bowne, V. Adler, K. A. Sookraj, V. Wu, V. Shteyler, H. Patel, W. Oxbury, P. Brandt-Rauf, M. E. Zenilman, J. Michl and M. R. Pincus, *Proc Natl Acad Sci U S A*, 2010, **107**, 1918-1923.
39. R. E. Moellering, M. Cornejo, T. N. Davis, C. Del Bianco, J. C. Aster, S. C. Blacklow, A. L. Kung, D. G. Gilliland, G. L. Verdine and J. E. Bradner, *Nature*, 2009, **462**, 182-188.
40. D. Raina, M. Kosugi, R. Ahmad, G. Panchamoorthy, H. Rajabi, M. Alam, T. Shimamura, G. I. Shapiro, J. Supko, S. Kharbanda and D. Kufe, *Mol Cancer Ther*, 2011, **10**, 806-816.
41. T. N. Grossmann, J. T. Yeh, B. R. Bowman, Q. Chu, R. E. Moellering and G. L. Verdine, *Proc Natl Acad Sci U S A*, 2012, **109**, 17942-17947.
42. M. L. Stewart, E. Fire, A. E. Keating and L. D. Walensky, *Nat Chem Biol*, 2010, **6**, 595-601.
43. B. Lin, S. K. Kolluri, F. Lin, W. Liu, Y. H. Han, X. Cao, M. I. Dawson, J. C. Reed and X. K. Zhang, *Cell*, 2004, **116**, 527-540.
44. P. M. Fischer, *Med Res Rev*, 2007, **27**, 755-795.
45. N. Kamaly, Z. Xiao, P. M. Valencia, A. F. Radovic-Moreno and O. C. Farokhzad, *Chem Soc Rev*, 2012, **41**, 2971-3010.
46. R. Z. Xiao, Z. W. Zeng, G. L. Zhou, J. J. Wang, F. Z. Li and A. M. Wang, *Int J Nanomedicine*, 2010, **5**, 1057-1065.
47. M. Kumar, D. Gupta, G. Singh, S. Sharma, M. Bhat, C. K. Prashant, A. K. Dinda, S. Kharbanda, D. Kufe and H. Singh, *Cancer Res*, 2014, **74**, 3271-3281.
48. S. Laurent, D. Forge, M. Port, A. Roch, C. Robic, L. Vander Elst and R. N. Muller, *Chem Rev*, 2008, **108**, 2064-2110.
49. O. Veisoh, J. W. Gunn and M. Zhang, *Adv Drug Deliv Rev*, 2010, **62**, 284-304.
50. T. K. Jain, M. A. Morales, S. K. Sahoo, D. L. Leslie-Pelecky and V. Labhasetwar, *Mol Pharm*, 2005, **2**, 194-205.
51. V. Mody, A. Cox, S. Shah, A. Singh, W. Bevins and H. Parihar, *Appl Nanosci*, 2014, **4**, 385-392.
52. L. Agemy, D. Friedmann-Morvinski, V. R. Kotamraju, L. Roth, K. N. Sugahara, O. M. Girard, R. F. Mattrey, I. M. Verma and E. Ruoslahti, *Proc Natl Acad Sci U S A*, 2011, **108**, 17450-17455.
53. G. Singh, N. H. Zaidi, U. Soni, M. Gautam, R. Jackeray, H. Singh and S. Sapra, *Journal of Nanoscience and Nanotechnology*, 2011, **11**, 3834-3842.
54. J. You, X. Li, F. de Cui, Y. Z. Du, H. Yuan and F. Q. Hu, *Nanotechnology*, 2008, **19**.
55. D. Brahatheeswaran, A. Mathew, R. G. Aswathy, Y. Nagaoka, K. Venugopal, Y. Yoshida, T. Maekawa and D. Sakthikumar, *Biomedical Materials*, 2012, **7**.

56. J. Zhou, C. Leuschner, C. Kumar, J. Hormes and W. O. Soboyejo, *Materials Science and Engineering: C*, 2006, **26**, 1451-1455.
57. M. M. Tomayko and C. P. Reynolds, *Cancer Chemotherapy and Pharmacology*, 1989, **24**, 148-154.
58. D. M. Euhus, C. Hudd, M. Laregina and F. E. Johnson, *Journal of Surgical Oncology*, 1986, **31**, 229-234.
59. D. F. Liu, W. Wu, X. Chen, S. Wen, X. Z. Zhang, Q. Ding, G. J. Teng and N. Gu, *Nanoscale*, 2012, **4**, 2306-2310.
60. T. W. Jacobs, A. M. Gown, H. Yaziji, M. J. Barnes and S. J. Schnitt, *J Clin Oncol*, 1999, **17**, 1974-1982.